

ARTICLE OPEN



TNF α increases tyrosine hydroxylase expression in human monocytes

Adithya Gopinath^{1,4}✉, Martin Badov^{1,4}, Madison Francis^{1,4}, Gerry Shaw^{1,2}, Anthony Collins¹, Douglas R. Miller¹, Carissa A. Hansen¹, Phillip Mackie¹, Malú Gámez Tansey¹, Abeer Dagra¹, Irina Madorsky², Adolfo Ramirez-Zamora³, Michael S. Okun^{1,3}, Wolfgang J. Streit¹ and Habibeh Khoshbouei¹

Most, if not all, peripheral immune cells in humans and animals express tyrosine hydroxylase (TH), the rate limiting enzyme in catecholamine synthesis. Since TH is typically studied in the context of brain catecholamine signaling, little is known about changes in TH production and function in peripheral immune cells. This knowledge gap is due, in part, to the lack of an adequately sensitive assay to measure TH in immune cells expressing lower TH levels compared to other TH expressing cells. Here, we report the development of a highly sensitive and reproducible Bio-ELISA to quantify picogram levels of TH in multiple model systems. We have applied this assay to monocytes isolated from blood of persons with Parkinson's disease (PD) and to age-matched, healthy controls. Our study unexpectedly revealed that PD patients' monocytes express significantly higher levels of TH protein in peripheral monocytes relative to healthy controls. Tumor necrosis factor (TNF α), a pro-inflammatory cytokine, has also been shown to be increased in the brains and peripheral circulation in human PD, as well as in animal models of PD. Therefore, we investigated a possible connection between higher levels of TH protein and the known increase in circulating TNF α in PD. Monocytes isolated from healthy donors were treated with TNF α or with TNF α in the presence of an inhibitor. Tissue plasminogen activator (TPA) was used as a positive control. We observed that TNF α stimulation increased both the number of TH⁺ monocytes and the quantity of TH per monocyte, without increasing the total numbers of monocytes. These results revealed that TNF α could potentially modify monocytic TH production and serve a regulatory role in peripheral immune function. The development and application of a highly sensitive assay to quantify TH in both human and animal cells will provide a novel tool for further investigating possible PD immune regulatory pathways between brain and periphery.

npj Parkinson's Disease (2021)7:62; <https://doi.org/10.1038/s41531-021-00201-x>

INTRODUCTION

Human and animal studies have shown that most if not all immune cells possess components necessary to release, uptake, synthesize, and respond to catecholamines including dopamine and norepinephrine (NOR). These components activate signaling cascades that change the phenotype and function of cells in both healthy and disease conditions. Immune cells may thus both come in contact with physiological levels of catecholamines derived from peripheral tissues and also serve as a source for catecholamines. Tyrosine hydroxylase (TH) catalyzes the conversion of tyrosine to 3,4-dihydroxyphenylalanine (L-DOPA), which is the rate-limiting step in the synthesis of dopamine, NOR, and epinephrine^{1,2}. Although primarily studied in the central nervous system (CNS)^{3,4}, TH is expressed in the majority of peripheral immune cells^{5–9}, and many peripheral tissues¹⁰, including kidney^{11,12}, heart¹³, and adrenal cortex^{14–16}. Both myeloid and lymphoid lineages of human peripheral immune cells express TH^{17,18}, which is thought to regulate dopamine levels within these cells⁹. Beyond protein expression, TH activity is regulated by a variety of post-translational modifications and can regulate TH function. For example, phosphorylation, ubiquitination, nitration, and S-glutathionylation can all affect TH activity independent of TH levels^{19–26}. As the key to catecholamine production, TH activity and its relative expression is commonly studied in diseases in which catecholamine tone, synthesis, and signaling are altered.

These disease states include bipolar disorder, addiction, schizophrenia, attention deficit hyperactivity (ADHD), and neurodegenerative conditions including Parkinson's disease (PD).

The lack of a robust and sensitive assay to measure low levels of TH protein has hampered the field's ability to investigate TH protein levels in peripheral immune cells in diseases characterized by altered catecholamine tone. For example, in PD, due to its spatially restricted expression, decreases in TH levels in the basal ganglia are readily detectable^{27,28}, whereas changes in TH levels in other brain regions (i.e., amygdala, hippocampus, cortical regions) are reported in the later stages of PD^{29,30}. In contrast, very low TH levels in countless immune cells spread across the body have made it difficult to study TH protein levels in peripheral immune cells. For example, indirect TH measurements via qPCR reveal that PD patients show significantly less midbrain TH mRNA compared to healthy controls subjects (5.5 ± 1.4 in healthy controls, vs. 1.5 ± 0.9 attomole/microgram total RNA in PD)³¹. In contrast, TH mRNA is not detectable in unstimulated immune cells³². TH protein expression in the substantia nigra is in excess of 200 ng TH per milligram protein³³ and is decreased in patients with PD. However, to our knowledge, no reports directly quantify TH protein in immune cells.

In order to investigate whether the characteristically reduced TH expression in PD CNS is recapitulated in peripheral immune cells, we established a sensitive assay to quantify TH protein. We then

¹Department of Neuroscience, University of Florida, Center for Translational Research in Neurodegenerative Disease, Norman Fixel Institute for Neurological Diseases, Gainesville, FL, USA. ²Encor Biotechnology Inc., Gainesville, FL, USA. ³Department of Neurology, University of Florida, Gainesville, FL, USA. ⁴These authors contributed equally: Adithya Gopinath, Martin Badov, Madison Francis. ✉email: adithya@ufl.edu

applied the assay to analyze TH production in peripheral blood monocytes. The sensitivity of our Bio-ELISA was a thousand-fold above traditional detection methods, and when we measured TH level in peripheral monocytes from healthy controls and from PD, we observed a significant elevation of TH levels in PD monocytes versus controls. This observation was contrary to our a priori hypothesis. The unexpected discovery of increased TH protein in peripheral PD monocytes prompted an investigation into the potential underlying mechanism. In the PD literature, there is a strong consensus that neuroinflammatory cytokines, including TNF α and IL6, are increased in CSF and serum of PD patients and of animal models of PD^{27,34–42}. Therefore, we investigated whether ex vivo exposure to TNF α or IL6 increases the number of TH+ monocytes and/or amount of TH protein per monocyte. We found that exposure to TNF α , but not IL6 increased both the number of TH+ monocytes and the quantity of TH protein per cell.

RESULTS AND DISCUSSION

Bio-ELISA successfully and reproducibly detects recombinant and native TH

To test the hypothesis that similar to CNS in PD, TH expression is reduced in peripheral blood monocytes, we first established a sensitive assay to quantify TH levels in monocytes from healthy controls, as well as various reference TH expressing systems. Given the plethora of biological systems expressing TH, there is an unmet need for a sensitive and reliable assay to quantify TH levels which with broad biological implications in basic science, preclinical and clinical research. To date, measurement of TH levels in midbrain neurons has been accomplished by immunohistochemistry, and Western blot^{43–46}, while TH levels in peripheral immune cells have been assayed by flow cytometry⁴⁷. Although reliable, these methods share a common shortcoming in that they are semi-quantitative at best, and at worst only indicate the presence or absence of TH. This led us to develop a highly sensitive and fully quantitative enzyme-linked immunosorbent assay (Bio-ELISA) to measure TH protein levels.

Quantification of TH using Bio-ELISA depends on the availability of purified TH and high-quality antibodies against TH, preferably generated in two distinct host species. A panel of monoclonal and polyclonal antibodies was generated against full-length recombinant human TH (Fig. 1a), and quality assessment was performed by standard ELISA, Western blotting, and appropriate cell and tissue staining. These novel antibodies behaved in all respects similar to a widely used commercial TH antibody (Fig. 1b, AB152, Millipore-Sigma)^{48–51}. A mouse monoclonal antibody, MCA-4H2, and a rabbit polyclonal, RPCA-TH, were selected as ELISA capture and detection antibodies, respectively.

Next, TH recombinant protein band identity was compared to TH expression in PC12 cells (Fig. 1c). As predicted, PC12 lysate shows a single TH band at ~63 kDa, with a corresponding band for the TH recombinant protein at ~70 kDa. The observed difference in molecular weight between TH expressed in PC12 cells and recombinant TH protein is due to the additional 5.7 kDa N-terminal His-tag. Lower molecular weight bands (at 50 and 35 kDa, Fig. 1b–e, Supplementary Fig. 1) represent proteolytic cleavage products of mammalian TH when expressed in a prokaryotic system. Both MCA-4H2 and RPCA-TH reliably detect both recombinant TH and native TH in PC12 lysates (Fig. 1c, d).

Since antibody specificity is crucial for developing a novel assay, we rigorously confirmed their specificity. First, MCA-4H2 and RPCA-TH were used to stain human and murine midbrain tissue (Fig. 2). MCA-4H2 (Fig. 2a) and RPCA-TH (Fig. 2b) both showed high specificity for TH+ dopamine neurons in both human and murine tissues with no visible background. In addition, both secondary-only and isotype control staining show minimal background (Fig. 2a, b, top and second panels). Lastly, both MCA-4H2

and RPCA-TH were tested via Western blot using standard immunoblotting as well as blocking peptide/absorption controls (Fig. 2c, d). Both antibodies show good specificity and minimal background. CHO cells, used as the negative control since they do not express TH, show no TH band (Fig. 2c). The peptide blocking/absorption control groups (Fig. 2d) also shows no detectable signal, further confirming specificity.

Next, we prepared 1:1 serial dilutions of TH recombinant protein in Laemmli buffer, from 6 to 0.094 μ g/mL, to test the limits of detection using the Licor IR imaging system for Western blot (Fig. 1e) using commercially available TH antibody AB152. While effective, detection via Licor Odyssey using an IR fluorescent dye affords a fixed lower detection limit of ~15 ng, suggesting that IR fluorescent imaging is suitable for high expressing systems, but unsuitable for accurate quantification at low nanogram or picogram TH levels, reinforcing the need for a more sensitive, quantitative TH Bio-ELISA.

To quantify TH expression in control conditions, we first attempted a standard sandwich ELISA approach (Fig. 1f), in which MCA-4H2 was used as the capture antibody, followed by incubation with recombinant TH, then RPCA-TH as the detection antibody. Enzyme-based detection was accomplished by the addition of HRP-conjugated secondary (goat anti-rabbit HRP, Vector, BA1000). While this reliably quantified TH, the standard version of this assay produced a lower detection threshold of 125 pg/mL TH. We sought to further increase the sensitivity of the assay by the addition of a biotin–avidin amplification step (Avidin-HRP, Vector, A2004) (Fig. 1g), which provided an improved lower threshold of 62.5 pg/mL. A further refinement was the biotinylation of the rabbit detection antibody using Sulfo-NHS-LC-biotin (Thermo Scientific A39257) which improved sensitivity further by reducing background and producing a lower-threshold of detection at 15 pg/mL (Fig. 1h) with biotinylated antibodies, hence the Bio-ELISA designation. We found that our Bio-ELISA is around one thousand-fold more sensitive than infrared Western blot imaging (15 pg/mL vs. 15 ng/mL). Both TH antibodies are available commercially from EnCor Biotechnology Inc.

Antibodies MCA-4H2 and RPCA-TH reliably detect both native and denatured TH in mouse and human tissue

Aiming to develop a novel and reliable ELISA for both human and murine tissues, we next sought to confirm the specificity of these antibodies on native and denatured tissues from both human and mouse brain regions rich in TH (Fig. 2). MCA-4H2 (Fig. 2a) and RPCA-TH (Fig. 2b) detect TH+ cell bodies and neuronal processes in both human and mouse midbrain. Minimal non-specific staining detected in secondary only and isotype controls, further confirming antibody specificity. Similarly, both MCA-4H2 and RPCA-TH detect denatured TH on Western blot (Fig. 2c) following separation on SDS–PAGE, with minimal non-specific bands in the negative control (parental CHO cell homogenate). HSP60 is shown as a loading control. As an additional validation step to confirm the specificity of MCA-4H2 and RPCA-TH, primary antibodies were pre-incubated with recombinant TH protein (blocking peptide/absorption control) and show no observable signal (Fig. 2d).

TH Bio-ELISA reliably quantifies TH in PC12 cells, human macrophages, and cultured murine dopamine neurons

Having established a reliable method with a suitably low detection threshold, we tested the TH Bio-ELISA on cell homogenates prepared from PC12 cells, HEK293 cells, cultured primary human macrophages derived from whole blood samples from healthy donors, and primary cultures of midbrain dopamine neurons prepared from PND0–PND3 mouse pups. PC12 cells are known to express high levels of TH⁵², while HEK293 serves as negative control^{53,54}. Cultured midbrain dopamine neurons are known to express TH as the rate-limiting enzyme for dopamine⁵⁵ while cultured human monocyte-derived macrophages express TH protein and mRNA^{9,56}.

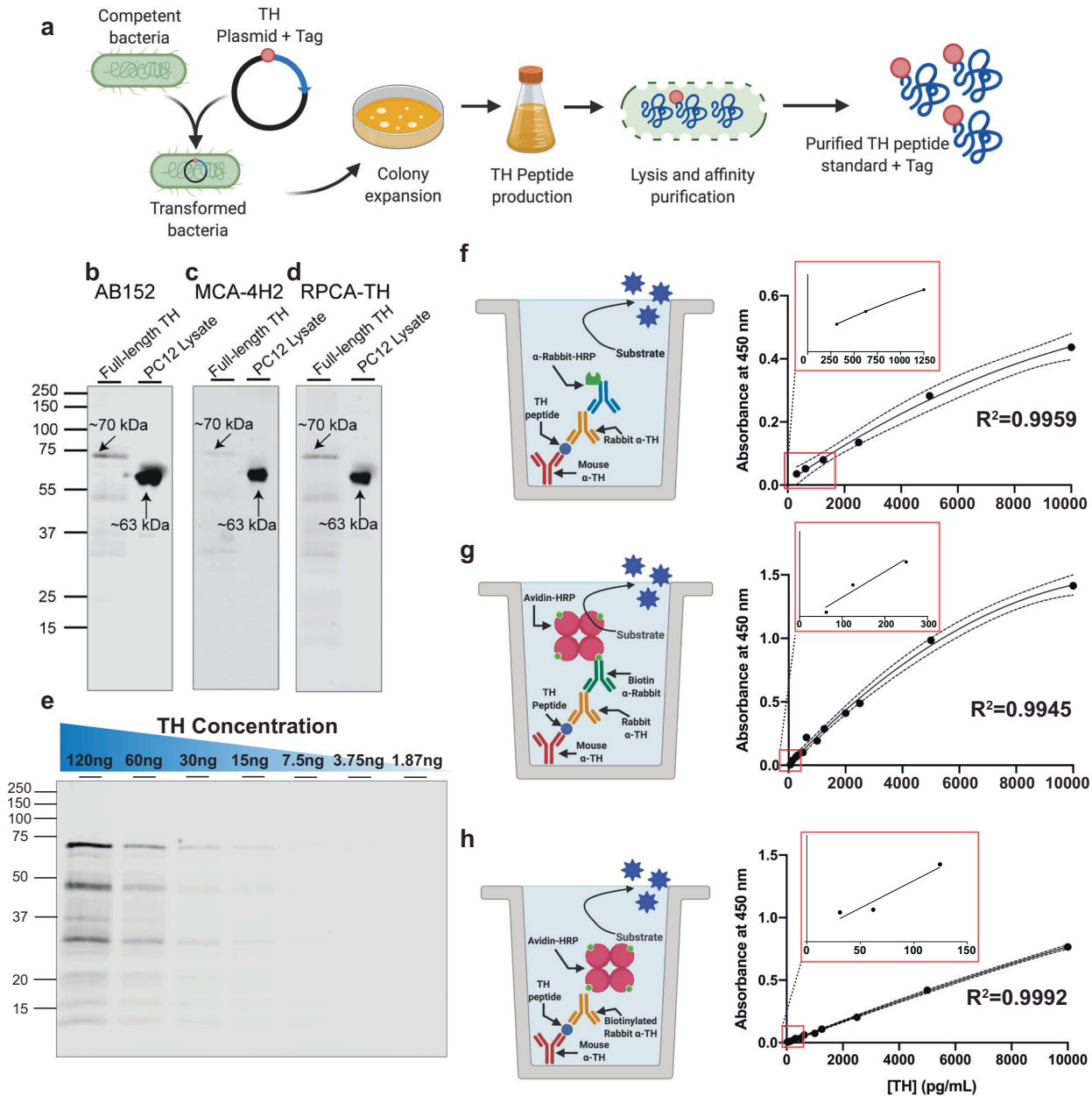


Fig. 1 Establishing a reproducible quantitative Bio-ELISA to detect tyrosine hydroxylase. **a–d** TH is detectable in recombinant form and in PC12 crude lysate using affinity-purified rabbit polyclonal TH antibody AB152 (Sigma), and antibodies selected for this ELISA, mouse monoclonal MCA-4H2 (EnCor), and rabbit polyclonal RPCA-TH (EnCor). **e** Using AB152, we probed the lower threshold for TH detection via serial dilution of purified recombinant TH from 6 to 0.094 $\mu\text{g}/\text{mL}$ followed by Western blot and near-infrared detection, considered to be a sensitive method for protein detection on Western blot. We demonstrate IR detection is reliable to a lower threshold of ~ 15 ng TH. Below this limit, TH detection becomes unreliable with IR detection. **f–h** In a series of stepwise experiments designed to increase ELISA sensitivity and decrease background, we achieved lower detection limits of 15 pg/mL TH (**h**). Capture antibody and detection antibody in all three methods were MCA-4H2 (1:1000 dilution from 1 mg/mL) and RPCA-TH (1:6000 dilution from 1 mg/mL). Schematic representation of each method shown on the left with a representative standard curve on the right. **f** Incubation with capture antibody followed by an HRP-conjugate secondary yielded a lower detection threshold of 125 pg/mL . **g** Addition of a tertiary layer using anti-rabbit biotin followed by Avidin-HRP improved lower detection threshold to 62.5 pg/mL but resulted in increased background. **h** Use of the biotinylated detection antibody (RPCA-TH-biotin, 1:6000 dilution from 1.65 mg/mL) followed by avidin-HRP yielded the lowest detection threshold of 15 pg/mL , with maximum sensitivity and minimal background. **f–h** Insets (red outline) shows a magnified lower standard curve to illustrate sensitivity.

TH expression is shown as unit TH (picogram or nanogram) per μg total protein, as determined by the Lowry assay. PC12 homogenate provided a reliable positive control expressing high levels of TH (>10 ng TH/ μg total protein), while HEK293 homogenate showed no detectable levels of TH, in at least six independent replicates. As anticipated, cultured dopamine neurons from postnatal mice showed greater TH concentrations (~ 700 pg TH/ μg total protein) than cultured

human macrophages (~ 300 pg TH/ mg total protein) (Fig. 3a), suggesting the Bio-ELISA is applicable to cell and tissue samples derived from human and murine specimens, paving the way for its application in translational and preclinical studies involving measurements of TH protein. We should note that, unlike cultured human monocyte-derived macrophages, cultured dopamine neurons contain various cell types, and consist of 12–16% dopamine neurons.

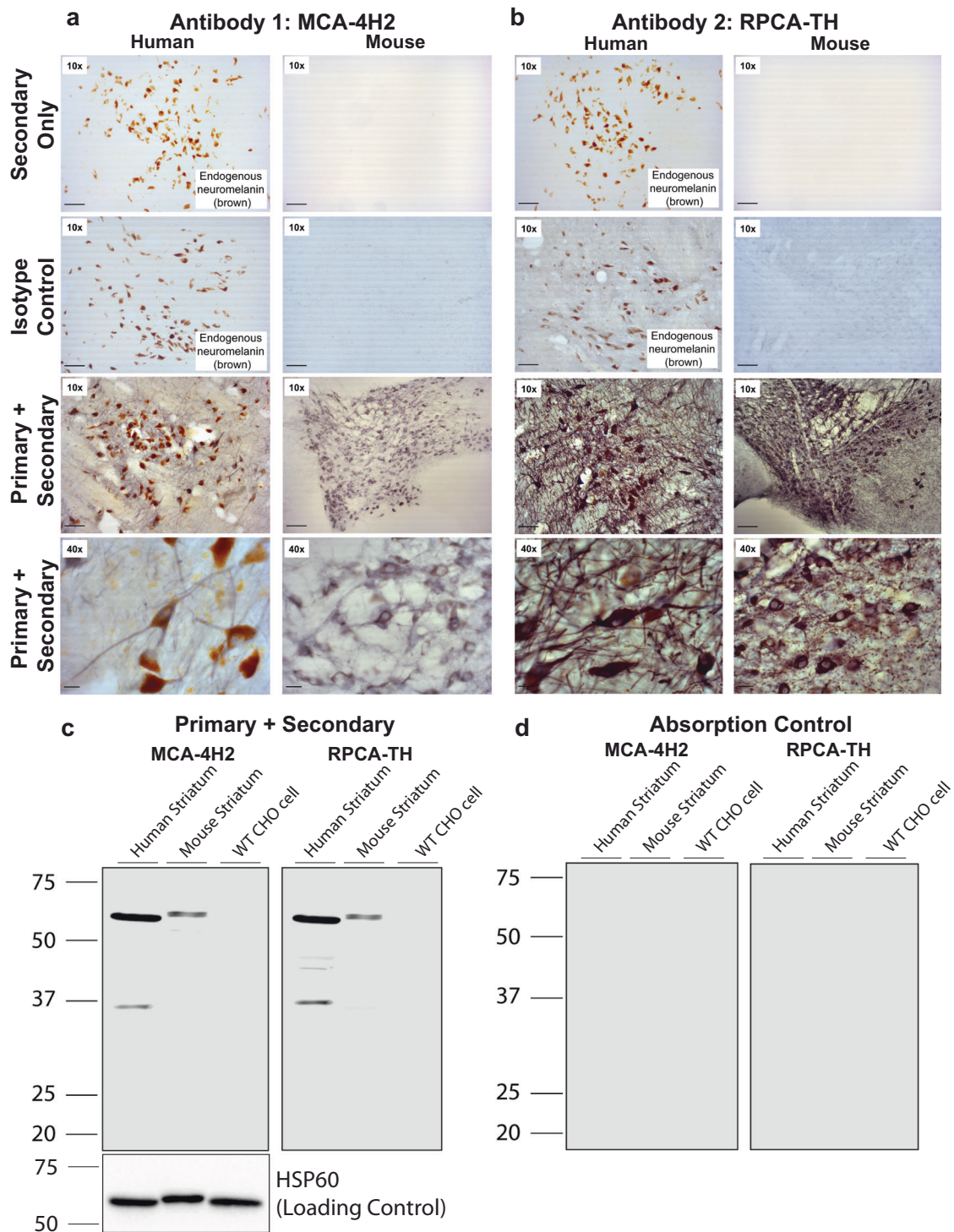


Fig. 2 Antibodies MCA-4H2 and RPCA-TH reliably detect both native and denatured TH in mouse and human tissue. Human and murine brain sections (40 μ m) were permeabilized, blocked, and stained with primary antibodies (MCA-4H2 and RPCA-TH) followed by HRP-conjugated secondaries and detected using diaminobenzidine enhanced with nickel (NiDAB, gray-black). **a** MCA-4H2 stains neuromelanin-expressing (brown) TH positive midbrain neurons and neuronal processes (gray-black) with no non-specific staining (secondary only, top panel; isotype control, second panel) in both human and murine tissues. **b** RPCA-TH shows similar highly specific staining of midbrain TH-positive neurons, confirming antibody specificity. **a** and **b** Human midbrain tissues showed as secondary-only and isotype controls exhibit endogenous neuromelanin (brown), not to be confused with immunostaining. **c** Western blot analyses of murine and human striatal tissues reveal similarly specific detection of TH (~63 kDa band) in both mouse and human, with minimal non-specific staining in negative control homogenate (parental CHO cell homogenate). (Left—MCA-4H2, right—RPCA-TH). **d** Blocking peptide/absorption control followed by western blot detection with either RPCA-TH and MCA-4H2 confirms the specificity of both antibodies for TH protein. HSP60 (loading control) is shown below and applies to **c** and **d**.

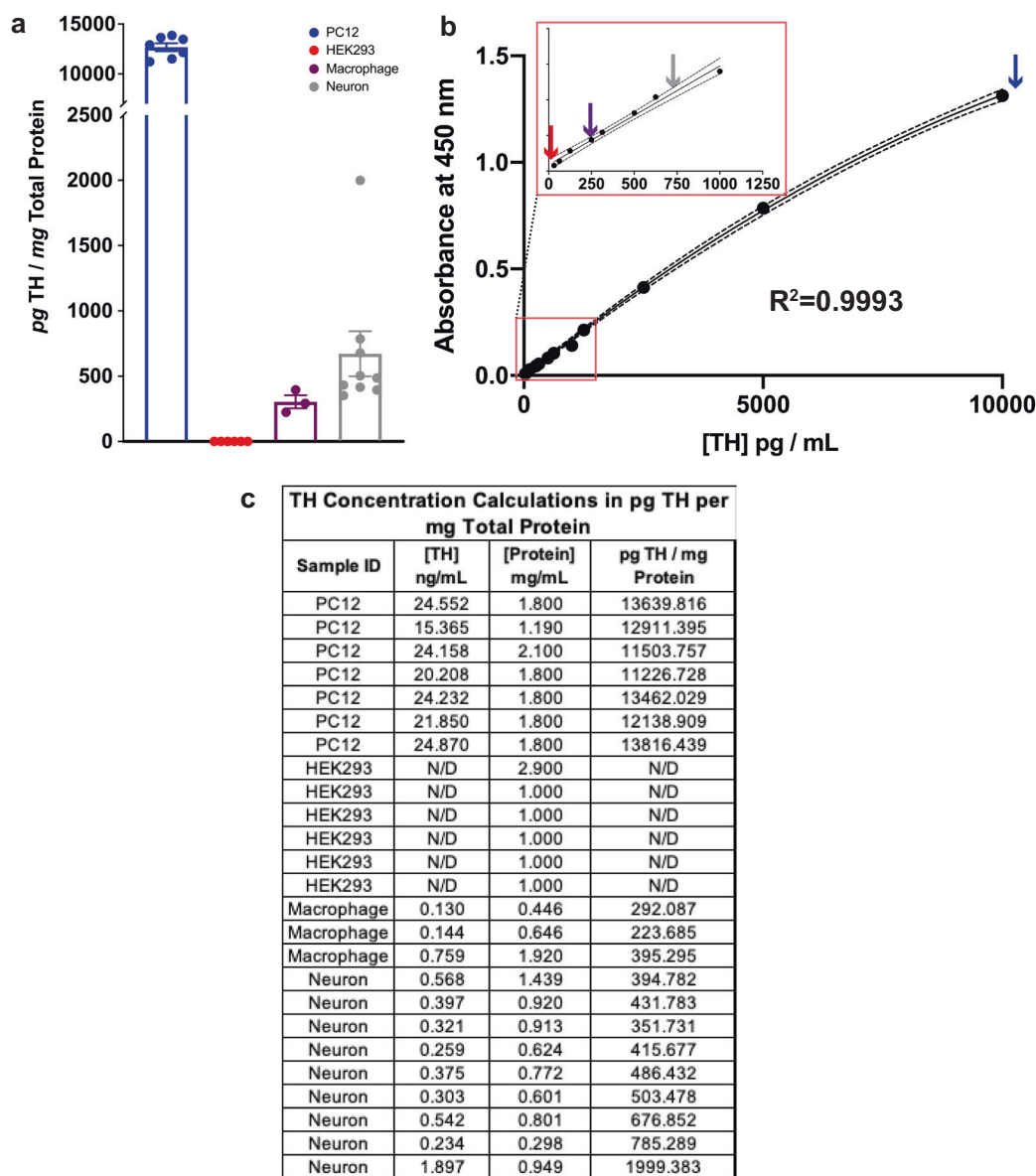


Fig. 3 Bio-ELISA reliably quantifies TH in PC12 cells, human macrophages and cultured murine dopamine neurons. **a** Using the Bio-ELISA shown in Fig. 1g, we quantified TH in four relevant tissues and cultured cells: PC12 (positive control), HEK293 (negative control), cultured human macrophages and cultured primary murine dopamine neurons. PC12 cells express very high levels of TH (<10 ng TH/mg total protein) relative to human macrophages (~300 pg TH/mg total protein) and primary murine dopamine neurons (~700 pg TH/mg total protein). **b** TH values are plotted on a representative standard curve for visual comparison, with an inset magnifying the lower end of the standard curve. **c** Calculations are shown by which raw TH concentration in ng/mL is normalized to total protein per sample. Samples included in **a**, each an independent biological replicate, are shown in **c**. Data are shown as \pm SEM.

The remainder is GABAergic neurons and supporting cells (microglia and astroglia)^{57–59}. Thus, we believe that TH levels are much higher in a single dopamine neuron than in a macrophage. Visual representation of relative TH expression in PC12, HEK293, human macrophage, and primary neuron homogenates are plotted on a representative standard curve (Fig. 3b). Raw values [TH] in ng/mL calculated from absorbance are shown in Fig. 3c, alongside each sample ID. Raw TH concentration was divided by [Protein], then multiplied by 1000 to produce values in pg TH/mg total protein (Fig. 3c).

To further confirm the specificity of these antibodies, the Bio-ELISA was tested using absorption controls (Fig. 4). In multiple independent replicates, a single ELISA plate was prepared as shown in Fig. 4a (Bio-ELISA, blue; absorbed MCA-4H2, orange; absorbed RPCA-TH, green), and incubated with PC12 lysate as a positive control. Following peptide blocking/absorption of either

capture or detection antibody, PC12 cell lysate yields no detectable TH (orange and green arrows, Fig. 4b), while the TH Bio-ELISA (blue arrow) recapitulates TH concentrations measured in PC12 cells (compare Fig. 3 panels a and b with Fig. 4 panel b).

Contrary to our hypothesis, monocytes isolated from the blood of PD patients show increased TH protein relative to age-matched healthy controls

PD is a disease in which monoamine signaling is affected in both CNS and peripheral immune cells⁹. The literature supports the hypothesis that similar to the CNS, peripheral TH expression is altered, but there is no reliable information about the direction of this change. Since peripheral immune cells including PBMCs express the machinery for catecholamine synthesis, including TH, they provide a biologically

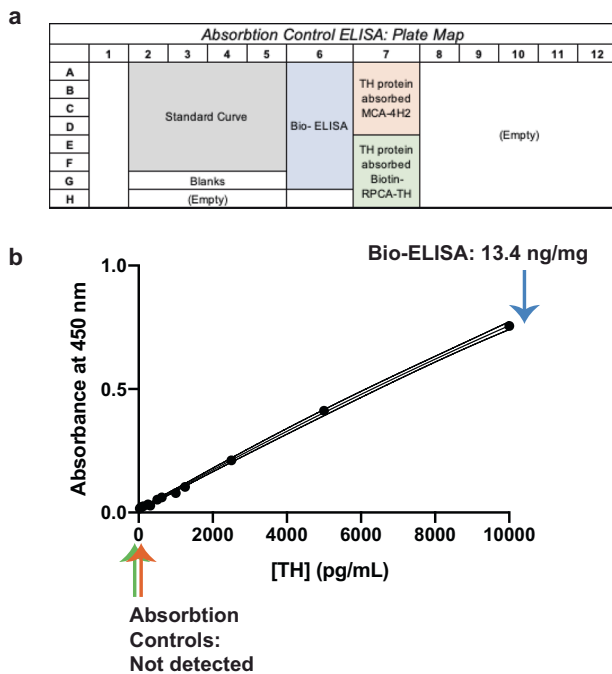


Fig. 4 Absorption controls demonstrate the specificity of TH Bio-ELISA. **a** Schematic layout of experimental conditions to assess absorption controls in contrast to optimized Bio-ELISA conditions using PC12 cell lysate. **b** Representative standard curve shown to illustrate PC12 cells' TH concentration using optimized Bio-ELISA (blue arrow), absorbed capture antibody (MCA-4H2 preincubated with 20 μ g/mL recombinant TH, orange arrow), and absorbed detection antibody (biotinylated RPCA-TH preincubated with 20 μ g/mL recombinant TH, green arrow). PC12 TH is undetectable after absorption of either capture or detection antibodies, confirming assay specificity.

relevant peripheral tissue preparation to investigate TH levels in monocytes of PD patients and age-matched healthy subjects. Monocytes for each subject were isolated from 20 million total peripheral blood mononuclear cells (PBMCs) using anti-CD14 magnetic isolation per the manufacturer's instructions. Purified monocytes were immediately lysed and assayed via Bio-ELISA for TH concentration following total protein quantification. Of 11 healthy control samples included, only three registered TH concentrations above the detection threshold. By contrast, all 11 PD patients recruited for this study show clear positive TH values that were significantly higher than healthy controls. These data suggest that, contrary to our original hypothesis, PD monocytes express significantly more TH protein relative to healthy control subjects (Fig. 5a— $n = 11$, $t[20] = 3.777$, $P = 0.0012$). Mean TH protein concentrations in PD monocytes are shown on a representative standard curve (Fig. 5b), along with raw data used to calculate TH concentrations (Fig. 5c). While these data represent a snapshot of TH levels in circulation PD monocytes, we cannot make any overarching claims that TH levels in monocytes precede clinical symptoms of PD, or predict a PD diagnosis. A larger sample number and longitudinal studies can test these possibilities. Nevertheless, these data suggest that in peripheral monocytes of Parkinson's patients, the rate-limiting protein involved in catecholamines synthesis is increased. Investigating the potential mechanism was the focus of the next set of experiments.

TNF α increases the number of TH $^{+}$ monocytes and the amount of TH protein per monocyte

There is strong evidence in the literature for increased TNF α in PD^{27,34–36} including in the brain, cerebrospinal fluid, and serum of

Parkinson's patients²⁷ as well as in Parkinsonian mice^{37,38}. These reports suggest that TNF α plays a role in the often hypothesized peripheral inflammation in PD^{60–65}, which is also documented in other inflammatory states including rheumatoid arthritis^{66,67} and multiple sclerosis⁷, where TH expression is linked to TNF α expression^{7,66,67}. Therefore, we tested the hypothesis that ex vivo stimulation of monocytes from healthy subjects with TNF α stimulates TH expression, as measured by changes in the number of TH-expressing monocytes, and/or the amount of TH per monocyte. We employed flow cytometry to address the former, and bio-ELISA to address the latter. Two million monocytes isolated from whole blood of healthy donors were treated for 4 h with tissue plasminogen activator (TPA, 100 ng/mL, positive control for increased monocyte TH expression⁷), TNF α (17 ng/mL)⁶⁸ and compared with monocytes treated with vehicle (Fig. 6a). Monocytes were assayed for TH expression by two complementary methods: flow cytometry⁴⁷ (Fig. 6b–f) and ELISA (Fig. 6g, h). We should note that because a prolonged TNF α exposure can induce cell toxicity^{69–73}, we tested multiple treatment durations. We found that a 4h TNF α (17 ng/mL)⁶⁸ treatment had a minimal effect on cell viability; whereas, a longer TNF α exposure substantially decreased cell viability. Therefore, a 4h treatment strategy was selected in this study.

To control for donor variability, we added identical quantities of counting beads as a reference. The number of TH $^{+}$ monocytes was quantified by flow cytometry (Fig. 6b, left) in two experimental groups: TPA-treated and TNF α -treated. Monocytes in each condition were gated to isolate single cells expressing TH (Fig. 6b). Raw counts of monocytes in each condition revealed increased monocytes expressing TH after treatment with TPA or TNF α (Fig. 6d), while the number of TH $^{+}$ monocytes per microliter (Fig. 6c) are significantly increased relative to vehicle (Fig. 6e; $N = 3$, $F(2,6) = 0.364$, $p = 0.0018$), suggesting that the number of TH $^{+}$ monocytes increases following treatment with TNF α or positive TPA control. A possible mechanism for this observation is either monocyte proliferation during the treatment period or an altered monocyte phenotype in response to TNF α , with no change in total number of monocytes. In other words, following TNF α treatment, TH $^{+}$ monocytes may either be increasing in number (proliferation) or existing monocytes upregulate TH expression and become TH $^{+}$ (phenotypic change). While a four-hour exposure to TNF α is an insufficient time period to induce proliferative events in immune cells⁶⁰, we could not confidently rule out these possibilities without additional analyses. Therefore, we quantified monocyte proliferation by comparing the total number of monocytes per microliter of untreated vs. TNF α -treated experimental group. We found the total number of monocytes per microliter to be unchanged (Fig. 6f). While these results suggest that monocyte proliferation did not occur in response to TNF α , the results of simple cell counts are not definitive. We elected to take a more rigorous approach and assess Ki67 expression as a measure of cell proliferation⁷⁴. Ki67 expression in TNF α -treated monocytes relative to vehicle-treated controls revealed no change in Ki67 expression following TNF α treatment (Fig. 6i). Thus, these results showed phenotypic changes in monocytes, but not cell proliferation in response to TNF α . While this finding explains our earlier observation of increased numbers of TH $^{+}$ cells, the potential phenotypic shift following TNF α -mediated immune stimulation was an unpredicted and novel finding.

Our flow cytometry data strongly support the conclusion that TNF α increases numbers of TH $^{+}$ monocytes, but an increased number of TH $^{+}$ monocytes could be due to increased numbers of cells expressing TH protein, increased quantity of TH protein per cell, or both. In order to determine whether or not TNF α treatment increases the quantity of TH protein per monocyte, identically treated monocytes were lysed and assayed using our TH Bio-ELISA. We found that four-hour treatments with TNF α significantly increased the amount of TH protein (picogram TH per milligram

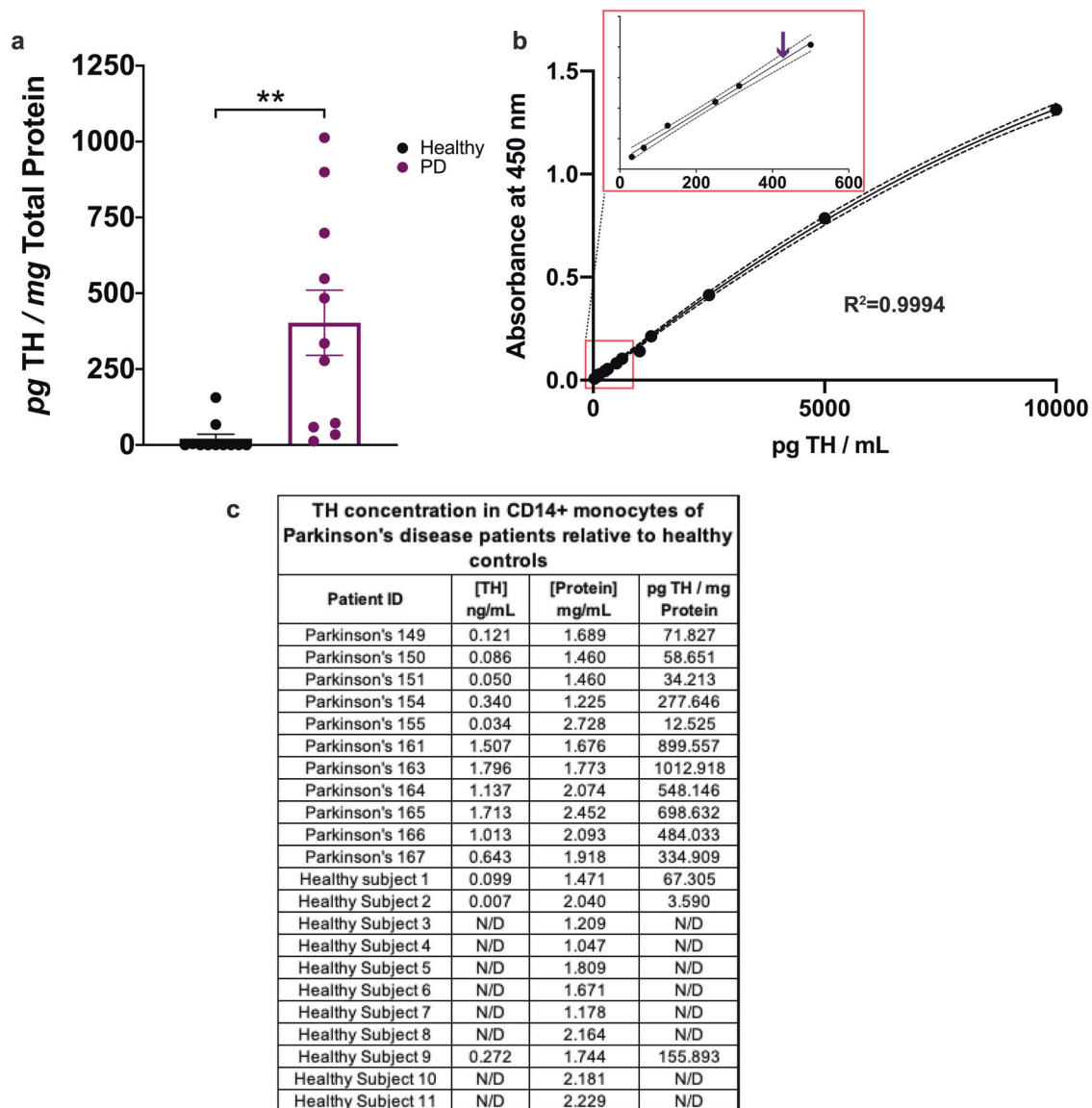


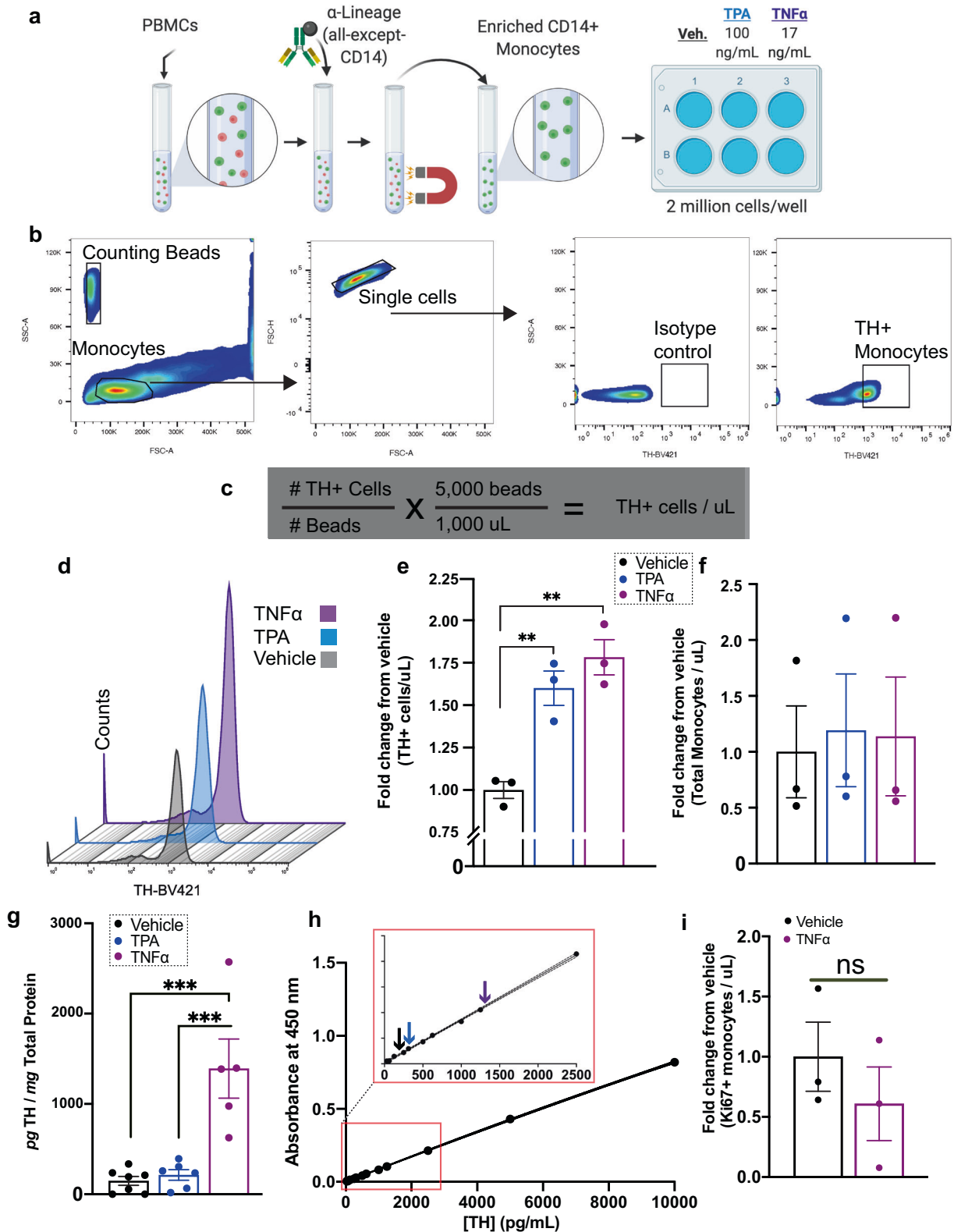
Fig. 5 TH protein is increased in CD14+ monocytes isolated from PD patients. Total CD14+ monocytes were magnetically isolated from 20 million freshly isolated PBMCs derived from whole blood of 11 PD patients and 11 healthy volunteers, immediately lysed in the presence of protease inhibitor, and stored at -80°C . Following protein quantification, the whole lysate from each sample was added to duplicate wells and assayed for the concentration of TH. **a** Monocytes isolated from PD patients express a significantly greater quantity of TH compared to equivalent monocytes isolated from healthy control subjects (unpaired two-tailed *T*-test, $\alpha = 0.05$, $p < 0.05$). **b** Mean TH concentration for monocytes from PD patients plotted on a representative standard curve, with inset magnifying the lower end of the curve. **c** Calculations are shown by which raw TH concentration in ng/mL is normalized to total protein per sample. Samples included in **a**, each an independent biological replicate, are shown in **c**. Data are shown as \pm SEM.

total protein) above both vehicle and the positive control group (TPA treatment; Fig. 6g; $n = 5-6$ per group, $F(2,15) = 3.297$, $p = 0.0001$), indicating that exposure to TNF α is sufficient to increase TH protein in human monocytes. Overall, our data show that TNF α increases both the number of monocytes-expressing TH and the quantity of TH expressed by each cell.

Inhibition of TNF α blocks increase in the number of TH+ monocytes and amount of TH per monocyte

To determine the specificity of TNF α regulation of TH in monocytes, we employed two approaches. We investigated whether inhibition of TNF α signaling attenuates or blocks the TNF α -mediated increase in TH. In addition, we asked whether or not interleukin-6 (IL6), a cytokine with pleiotropic effects⁵⁷ that is also increased in PD⁷⁵⁻⁷⁷

and is associated with non-motor symptoms of PD⁷⁵⁻⁷⁷ can also regulate TH expression in the peripheral monocytes. To test these possibilities, we investigated whether XPro1595, a TNF α inhibitor^{78,79}, reduces monocyte TH expression relative to TNF α treatment alone. In parallel experiments, monocytes were treated with IL6. Two million monocytes isolated from the whole blood of healthy donors (Fig. 7a) were treated with XPro1595 alone (50 ng/mL), TNF α (17 ng/mL), or TNF α plus XPro1595 (Fig. 7b), IL6 alone (17 ng/mL) or IL6 plus XPro1595. The cells were subjected to flow cytometry or Bio-ELISA. Consistent with the literature⁵⁷, we found relative to TNF α treatment alone, XPro1595 inhibition of TNF α reduced both the number of TH+ monocytes and the quantity of TH per monocyte (Fig. 7c, d), suggesting that soluble TNF α mediates increased TH in human monocytes. As shown in Fig. 7c, d, IL6 neither changed the number of TH+ monocytes nor the quantity of TH per monocyte. We should



note that our data show that TNF α is capable of regulating TH in monocytes whereas other elevated cytokines, including IL6, are not. Since we have not tested the effect of additional, non-upregulated cytokines, we cannot claim that what we have shown in this study is exclusively mediated by TNF α . Instead, we only claim that TNF α is

capable of regulating monocyte TH. In addition, while we have not investigated the direct link between increased TH protein in PD monocytes and TNF α , our ex vivo data (Fig. 6) support the interpretation that TNF α plays a role in increased TH expression in immune cells of PD patients.

Fig. 6 TNF α increases the number of TH⁺ monocytes and the amount of TH protein per monocyte. **a** Total of CD14⁺ monocytes were isolated using a negative magnetic selection from 80 million healthy donor PBMCs. Monocytes were seeded into a six-well ultra-low-adherence plate at 2 million cells per well and treated with vehicle (media), TPA (100 ng/mL, positive control), TNF α (17 ng/mL), in duplicate. **b** One duplicate was assayed by flow cytometry to detect TH-expressing monocytes, using counting beads as a reference value to quantify the number of TH⁺ cells. **c** Number of TH⁺ cells were quantified as shown. **d** Representative histogram showing one set of samples assayed for TH-expressing monocytes following stimulation. **e** Both TPA and TNF α induced significant increases in TH-expressing monocytes relative to vehicle, shown as fold-increase relative to vehicle ($n = 3$ per group, one-way ANOVA, $p < 0.01$). **f** No increase in total monocytes per condition, relative to vehicle ($n = 3$ per group, one-way ANOVA, n.s.). **g** TH concentration in picograms per milligram total protein shows TNF α treatment results in significantly increased TH protein relative to vehicle and TPA ($n = 5-6$ per group, one-way ANOVA, $p < 0.001$). **h** Mean TH protein level for monocytes treated with vehicle, TPA and TNF α are plotted on a representative standard curve, with the inset magnifying the lower end of the curve. **i** Intracellular flow cytometry for Ki67 does not reveal significant differences between vehicle and TNF α treatment groups, confirming a lack of cell proliferation following TNF α treatment. Data are shown as \pm SEM.

In summary, we developed a highly reproducible and quantitative Bio-ELISA to measure TH protein levels in murine and human cells. Following validation of our assay in multiple TH expression systems, we investigated TH expression in PD immune cells and of age-matched healthy control subjects. We observed that PD patients' monocytes expressed significantly greater amounts of TH per monocyte. Inspired by the literature indicating increased TNF α in PD, we uncovered an intriguing link between TNF α stimulation and increased TH expression in healthy monocytes, which is attenuated by treatment with TNF α inhibitor Xpro1595. Given that TH expression and catecholamine release has been shown to be associated with an anti-inflammatory effect and can mitigate TNF α mediated inflammation, we posit that increased TH expression in monocytes in response to elevated TNF α is a compensatory mechanism. This observation is a step towards understanding the potential underlying mechanism and functional consequence of changes in catecholamines in peripheral immune system in PD. Nevertheless, we acknowledge that one of the limitations of this study was the infeasibility of quantifying TNF α responses in PD monocytes. Whereas, TH can be quantified in a 30 mL blood sample (Figs. 3–5), for functional assays (Figs. 6 and 7) a large blood volume (~500 mL) is required, which is not feasible in PD subjects. In addition, our data represent merely a snapshot of TH levels present in circulating PD monocytes at a single timepoint; we do not make any claims that elevated levels of TH expressing monocytes precede or predict PD. Larger sample numbers and longitudinal studies can test these possibilities. Nonetheless, the current results raise many interesting questions: Do the circulating TH expressing monocytes reflect changes in central dopamine? Does effective PD therapy reduce the level of TH in peripheral immune cells? Does elevated TH in monocytes predict PD onset or its progression? Future studies will examine these questions and the connections between the peripheral immune system to the brain.

METHODS

Human subjects

Human brain tissues were obtained via approved IRB protocols #IRB201800374 and IRB202002059 respectively. Blood samples were obtained at the University of Florida Center for Movements Disorders and Neurorestoration according to an IRB-approved protocol (#IRB201701195).

Brain tissues from healthy subjects

Human brain tissues were obtained via approved IRB protocols IRB202002059 and IRB201800374, from the UF Neuromedicine Human Brain and Tissue Bank (UF HBTB). The tissues were not associated with identifying information, exempt from consent, therefore no consent was required. Regions of interest were identified and isolated by a board-certified neuropathologist.

Blood samples from healthy subjects

Blood samples from age-matched healthy subjects were obtained from two sources: an approved IRB protocol with written informed consent (IRB201701195), or were purchased from Lifesouth Community Blood Center, Gainesville, FL from August 2017 to January 2020 as deidentified samples, and exempt from informed consent (IRB201700339). According to Lifesouth regulations, healthy donors were individuals aged 50–80 years-old of any gender, who were not known to have any blood borne pathogens (both self-reported and independently verified), and were never diagnosed with a blood disease, such as leukemia or bleeding disorders. In addition, none of the donors were using blood thinners or antibiotics, or were exhibiting signs/symptoms of infectious disease, or had a positive test for viral infection in the previous 21 days.

Blood samples from PD patients

Blood samples were obtained from PD patients (aged 50–80 years-old of any gender) at the University of Florida Center for Movements Disorders and Neurorestoration according to an IRB-approved protocol (#IRB201701195), via written informed consent. All recruited patients' PD was idiopathic. Patients did not have any recorded blood-borne pathogens or blood diseases, nor were they currently taking medications for infections according to their medical record. In addition, none of the donors were using blood thinners (warfarin, heparin), antibiotics, over-the-counter (OTC) medications other than aspirin, or were exhibiting signs/symptoms of infectious disease or had a positive test for viral infection in the previous 21 days. Current medications are summarized in Supplementary Table 1.

TH recombinant protein

Full length human TH protein was expressed from a synthetic cDNA inserted into the *EcoRI* and *Sall* sites of the pET30a(+) vector and was codon optimized for expression in *E. coli*. The vector adds an N-terminal His-tag and other vector sequence, a total of 5.7 kDa. Expression of the construct was made by standard methods and purification was performed using the His tag by immobilized metal affinity chromatography on a nickel column. The TH sequence used in this study is the human tyrosine 3-monoxygenase isoform shown in Uniprot entry P07101-2.

MODEL SYSTEMS USED FOR THE VALIDATION OF BIO-ELISA

Human macrophages

Primary human macrophages were cultured as described previously⁵⁶. PBMCs isolated as described below were re-suspended in RPMI 1640 containing 1% Pen/Strep and 7.5% sterile-filtered, heat-inactivated autologous serum isolated from the donor's own blood, and plated in 24-well untreated polystyrene plates at 1 million PBMCs per well. To retain only monocytes/macrophages, cells were washed after 90 min of adherence time to remove non-adherent cells with incomplete RPMI 1640, followed by replacement with complete media. Media was replaced at days 3 and 6 following culture, and cell lysis performed on day 7 following culture.

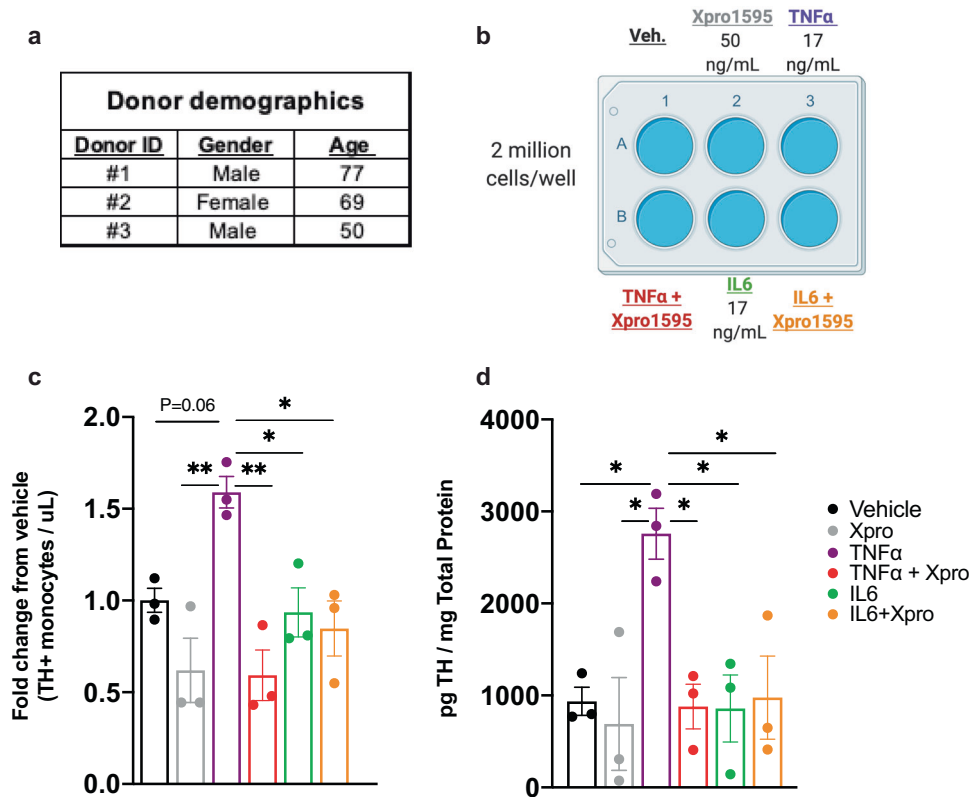


Fig. 7 Inhibition of TNF α blocks increase in number of TH $^{+}$ monocytes and amount of TH per monocyte. **a** and **b** Acutely isolated monocytes from three healthy donors were seeded at 2 million cells per well in duplicate ultra-low-adherence plates, and treated with TNF α (17 ng/mL), XPro1595 (50 ng/mL), IL6 (17 ng/mL) or combinations thereof as indicated. **c** In samples assayed by flow cytometry, using counting beads as a reference value to quantify the number of TH $^{+}$ cells, co-incubation with TNF α and XPro1595 significantly reduced the number of TH $^{+}$ monocytes relative to TNF α treatment alone. Treatment with IL6 or IL6 + XPro1595 resulted in no significant change in the number of TH $^{+}$ monocytes. Values are represented as fold change relative to vehicle ($n = 3$ per group, one way ANOVA, $*p < 0.05$, $**p < 0.01$). **d** TH concentration (picogram per milligram total protein) significantly increases upon TNF α treatment, and is reduced significantly to baseline levels following co-incubation with TNF α and XPro1595. Neither IL6 nor IL6 + XPro1595 significantly increased TH quantity ($n = 3$ per group, one way ANOVA, $*p < 0.05$). Data are shown as \pm SEM.

Primary murine midbrain dopamine neurons

Midbrain dopamine neurons strongly express TH⁸⁰ and were used as a positive control group. Animal studies were performed in compliance with University of Florida IACUC ethical regulations and rules (IACUC# 201808953). Acutely dissociated mouse midbrains from 0–2 day-old male and female pups were isolated and incubated in dissociation medium at 37 °C under continuous oxygenation for 90 min. Dissociated cells were pelleted by centrifugation at 1,500 $\times g$ for 5 min and resuspended and triturated in glial medium (Table 1). Cells were then plated on 12 mm coverslips coated with 0.1 mg/mL poly-D-lysine and 5 μ g/mL laminin and maintained in neuronal media. Every 4 days, half the media was replaced with fresh media. The materials used for the preparation and maintenance of midbrain neuronal culture are outlined in Table 1.

Positive and negative control cell lines

All cell cultures were maintained at 37 °C with 5% CO₂ and all cell culture supplies are listed in Table 2. HEK293 cells⁵³ are not thought to express TH and so were used as a negative expression control and were cultured as described previously^{55,81}. PC12 cells express TH⁵² and were used as a positive control. The cells were cultured as described by Cartier et al. 2010⁴⁹. CHO cells were cultured as previously described⁸², and were used as a negative control for TH expression.

PBMC isolation

PBMCs express TH^{47,56}. As previously published⁴⁷, whole blood was collected in K2EDTA vacutainer blood collection tubes (BD, 366643) and held at room temperature for up to 2 h prior to PBMC isolation. Briefly, blood from healthy volunteers and PD patients was overlaid in Leucosep tubes (Table 2) for PBMC isolation, centrifuged for 20 min at 400 $\times g$ with brakes turned off and acceleration set to minimum. PBMCs were collected from the interphase of Ficoll and PBS, transferred to a fresh 15 mL conical tube, resuspended in 8 mL sterile PBS and centrifuged for 10 min at 100 $\times g$, and repeated twice more. Cells were counted with a hemacytometer using trypan blue exclusion of dead cells, and density-adjusted for downstream applications.

Magnetic monocyte isolation

PBMCs are composed of multiple cell subsets⁸³, each with distinct function and catecholamine sensitivity^{84,85}—for example, lymphocyte regulation by catecholamines dopamine and NOR^{5,6,86} have been studied for several decades^{8,18,87,88}, while data regarding catecholamine function in myeloid lineage cells including monocytes is less abundant. In this study, we were narrowly focused on studying peripheral monocytes which we and others have previously shown to express TH^{9,47,89–91}. Because PBMCs comprise a variety of immune cell types, we used immunomagnetic enrichment to obtain a greater than 95% CD14 $^{+}$ monocytes that were utilized in assays described in the current study. Supplementary Fig. 2 shows representative flow

Table 1. Neuron culture reagents.

Dissociation media			
Chemical name	Concentration	Vendor	Catalog number
NaCl	116 mM	Sigma-Aldrich	S7653
NaHCO ₃	26 mM	Sigma-Aldrich	D6546
NaH ₂ PO ₄	2 mM	Sigma-Aldrich	S9638
D-glucose	25 mM	Sigma-Aldrich	G8769
MgSO ₄	1 mM	Sigma-Aldrich	M7506
Cysteine	1.3 mM	Sigma-Aldrich	C7352
Papain	400 units/mL	Worthington	LS003127
Kynurenic acid	0.5 mM	Sigma-Aldrich	K3375
Glial media			
DMEM	51.45	Thermo Fisher Scientific	11330032
Fetal Bovine Serum	39.60	Gemini	100-106
Penicillin/ Streptomycin	0.97	Thermo Fisher Scientific	15-140-122
Glutamax 100x	0.97	Thermo Fisher Scientific	35050061
Insulin (25 mg/ mL stock)	0.08	Sigma-Aldrich	I5500
Neuronal Media			
Neurobasal-A	96.9	Thermo Fisher Scientific	10888022
B27 Plus	1.9	Thermo Fisher Scientific	A3582801
GDNF	0.97	Sigma-Aldrich	SRP3200
Glutamax 100x	0.15	Thermo Fisher Scientific	35050061
Kynurenic acid	0.08	Sigma-Aldrich	K3375

cytometry data from routine verification of monocyte enrichment. (Supplementary Fig. 2)⁹².

CD14⁺ monocytes express TH⁴⁷. Primary CD14⁺ monocytes were isolated using Biolegend MojoSort magnetic isolation kit (Biolegend, 480094) per manufacturer's instructions. Briefly, 20 million total PBMCs were counted, density adjusted to 1 million cells/ μ L, resuspended in MojoSort buffer, and incubated with TruStain Fc-block for 10 min at room temperature, followed by 1:10 anti-CD14 magnetic nanobeads for 15 min on ice. Following 2 washes with 2.5 mL ice-cold MojoSort buffer, cell pellet was resuspended in 2.5 mL MojoSort buffer and subject to three rounds of magnetic isolation per manufacturer's instructions. The resulting cell pellet was washed to remove remaining non-CD14⁺ cells and subject to cell lysis as detailed below.

Preparation of cell lysates

Adherent cells in culture were lifted using 0.02% EDTA in PBS, diluted with 5 volumes of PBS, and centrifuged at 100 \times g. Non-adherent cells (PC12) were centrifuged at 100 \times g for 5 min at room temperature, and cell pellets were washed three times with 5 volumes of sterile PBS. Primary macrophages and primary murine neuron cultures were washed thrice with ice-cold PBS, on ice. Cell pellets and adherent primary cells were then lysed in ice-cold lysis buffer (10 mM NaCl, 10% glycerol (v/v), 1 mM EDTA, 1 mM EGTA, and HEPES 20 mM, pH 7.6), with Triton X-100 added to a final concentration of 1%, containing 1 \times protease inhibitor cocktail (Millipore-Sigma, 539131) for one hour at 4 °C with rotation. Resulting lysate was centrifuged at 12,000 \times g for 15 min

Table 2. Equipment.

Equipment	Supplier	Part number	Purpose
Centrifuge	Eppendorf	5424R	Cell lysate centrifugation
Centrifuge	Sorvall	ST8	Cell culture
Magnet	Biolegend	480019	Magnetic Isolation
Plate reader	Biorad	iMark	WB/ELISA
Odyssey	Licor	Odyssey	WB
ChemiDoc+	Biorad	ChemiDoc MP	WB
Mini-Protean Tetra	Biorad	1658005	WB
ELISA shaker	VWR		ELISA incubations
Plate Washer	BioTek	ELX-405	ELISA washes
Spectral Analyzer	Sony	SP6800	FC

at 4 °C. Supernatant was set aside for protein quantification by Lowry assay (Biorad, 5000112) and the remainder was stored at -80 °C until use for downstream assays.

Western blot

Reagents, antibodies and equipment are outlined in Tables 2, 3 and 4. Samples of PC12 lysate (5 μ g) and recombinant TH protein (120, 60, 30, 15, 7.5, 3.75, and 1.875 ng) were incubated in Laemmli sample buffer containing 10% beta-mercaptoethanol at 37 °C for 30 min, separated by SDS-PAGE on 10% bis/polyacrylamide gels, and transferred to nitrocellulose membranes. After first blocking for 1 h in TBS-T (50 mM Tris-HCl, 150 mM NaCl, and 0.1% Tween 20) containing 5% dry milk (blocking buffer), then incubated with primary antibody against TH (Table 4) overnight at 4 °C. Membranes were then incubated with an appropriate secondary antibody (Table 4) for 1 h at room temperature with agitation. Following all antibody steps, membranes were washed three times for 5 min each using TBS-T. TH was visualized using the Licor Odyssey (Table 2). Absorption controls were performed as follows: the primary antibodies were pre-incubated with 20 μ g/mL recombinant TH protein for 30 min on ice, then were used to confirm primary antibody specificity (Table 3, Fig. 2c, d).

Immunohistochemistry

Human tissues were sectioned at 40 μ m on a vibrating microtome and subjected to antigen retrieval in citrate buffer (10 mM citric acid, 2 mM EDTA, 2% Tween-20, pH 6.2) at 96 °C for 30 min, and then allowed to cool to room temperature. PFA-perfused mouse brain tissues were also sectioned at 40 μ m on a vibrating microtome.

Human and murine brain tissues were quenched for 20 min with 3% hydrogen peroxide, blocked and permeabilized at 37 °C for 1 h in PBS containing 5% normal goat serum and 0.5% TritonX-100. Primary antibodies RPCA-TH and MCA-4H2 (1:500 and 1:100 dilution, respectively, Table 4) were incubated overnight, followed by secondaries conjugated to HRP (1:250, Table 4), incubated for 1 h at room temperature. Isotype control antibodies (Biolegend, Table 1) were used to confirm the specificity of RPCA-TH and MCA-4H2. Sections were detected with HRP-substrate NiDAB (Vector Labs, Table 3).

Detection antibody (RPCA-TH) biotinylation

EZ-Link Sulfo-NHS-LC-Biotin (A39257, Thermo Scientific) at 20-fold molar biotin was used according to the manufacturer's protocol. Anti-biotin antibody was concentrated to 2 mg/mL, pH was adjusted to 8.0 at room temperature. The conjugate was purified

Table 3. Reagents and Materials.

Reagent	Supplier	Catalog number	Purpose	Concentration
EZ-Link Sulfo-NHS-LC-Biotin	Thermo Scientific	A39257	RPCA-TH biotinylation	20-fold molar excess
Fat-free milk	Carnation	N/A	WB/ELISA	1% or 5%
Clarity Western	BioRad	1705061	WB ECL	N/A
TMB Substrate	ThermoFisher	34028	ELISA	Stock
NiDAB	Vector Labs	SK-4100	IHC	Stock
TPA	Biologend	755802	ELISA, FC	100 ng/mL
IL6	Biologend	570802	ELISA, FC	17 ng/mL
TNF-alpha	Biologend	570102	ELISA, FC	17 ng/mL
H2SO4	Sigma	339741	ELISA	2 N
TritonX-100	ThermoFisher	BP151-100	Magnetic Isolation	1%
Tween-20	ThermoFisher	MP1Tween201	TBS-T	0.2%
Protease Inhibitor	Millipore	539191	Cell lysis	1×
DC Protein assay	Biorad	5000112	Protein assay	N/A
FBS	Gemini	100-106	Cell culture	10% or 5%
Horse serum	Sigma	H1138-500ML	Cell culture	5%
Pen/Strep	ThermoFisher	15-140-122	Cell culture	1%
RPMI	Corning	10-017	Cell culture	Stock
Immulon 4HBX	ThermoFisher	3855	ELISA	N/A
MojoSort buffer 5x	Biologend	480017	Magnetic cell isolation	1×
Leucosep tubes	Grenier BioOne	227290P	PBMC isolation	N/A
Ultra-low-adherence 6-well plates	Corning	3471	TPA/TNF-alpha stimulation in vitro, for ELISA/FC	N/A
Accumax	Innovative Cell Tech	AM105	Cell detachment	Stock
CountBright beads	Invitrogen	C36950	FC	5000 beads/ μ L
XPro1595	N/A	N/A	In vitro treatment	50 ng/mL

by gel filtration on a Biorad 10DG column (cat 732-2010) at room temperature.

ELISA for TH

Antibodies used for ELISA are described in Table 1. Ten lanes of an Immulon 4 HBX High-Binding 96-well plate were coated with 100 μ L per well of 1:1000 dilution of 1 mg/mL mouse anti-TH (MCA-4H2) in coating buffer (28.3 mM Na_2CO_3 , 71.42 mM NaHCO_3 , pH 9.6) for 20 h at 4 °C. Edge lanes 1 and 12 were left empty. Wells were blocked with 5% fat free milk in 1× TBS (pH 7.4) for 1 h at room temperature on an orbital shaker set to 90 rpm. To produce a standard curve, two standard curve lanes were generated, with six serial dilutions, beginning at 10 ng/mL and 1 ng/mL in TBS-T containing 1% fat free milk (with the last well in each standard curve lane left with incubation buffer only as a blank. Remaining wells were incubated in duplicate with 100 microliters of lysates from 1.5 million cells of interest. Incubation was completed for 20 h at 4 °C on an ELISA shaker set to 475 rpm.

After each well was washed and aspirated six times with TBS-T, affinity purified polyclonal rabbit anti-TH (EnCor, RPCA-TH) conjugated to biotin was diluted 1:6000 from a stock concentration of 1.65 mg/mL in TBS-T with 1% fat-free milk and incubated for 1 h at room temperature at 425 rpm. 100 μ L Avidin-HRP (Vector labs, A-2004), diluted 1:2500 in TBS-T with 1% fat-free milk, was added to each well following washing as described above, and incubated for 1 h at room temperature at 425 rpm. Following final washes, 150 μ L room temperature TMB-ELISA reagent (Thermo Fisher, 34028) was added to each well. The reaction was allowed to continue for 20 min, protected from light, and stopped by the addition of 50 μ L 2 N H_2SO_4 . The plate was immediately read at 450 nm. Absorption controls (Fig. 4) were conducted by

pre-incubating MCA-4H2 and RPCA-TH with a 20-fold excess concentration of recombinant TH protein for 30 min on ice, prior to addition to the ELISA plate, followed by the remainder of the protocol described above.

Duplicate standard and sample wells were averaged and background-subtracted based on blank wells. The concentration of TH for each experimental group was calculated using a quadratic curve equation calculated in Graphpad Prism 8, then normalized to total protein concentration per sample as calculated using the Lowry assay. Samples that produced negative values for TH concentration were considered below the detection threshold, and therefore assigned a value of 0. Final TH values shown are presented as pg TH/mg total protein after the multiplication of the nanogram TH value by 1000 to show TH as picogram TH/milligram total protein.

In vitro stimulation/treatment with TNF α , tissue plasminogen activator (TPA), TNF α inhibitor XPro1595 and IL6

Monocytes were isolated from total PBMCs prepared as described above⁴⁷ using negative selection (Biologend, 480048) per manufacturer's instructions. Total PBMCs were Fc-blocked to reduce nonspecific binding, followed by incubations with biotin-conjugated antibody cocktail containing antibodies against all subsets except CD14 (negative selection), followed by incubation with magnetic-Avidin beads, allowing all subsets other than CD14 + monocytes to be bound to the magnet. Monocyte purity/enrichment was routinely verified to confirm that the final cell population was >95% pure CD14+ cells (Fig. S2). CD14+ monocytes were collected from the supernatant fraction, washed, counted, and density adjusted such that 2 million CD14+ monocytes were seeded per well (Fig. 5a) and treated for 4 h

Table 4. Antibodies.

Specificity	Clone/species	Conjugate	Vendor	Catalog number	Purpose	Dilution	Concentration ($\mu\text{g}/\text{mL}$)
TH	Polyclonal/Rabbit	N/A	Sigma	AB152	WB	1:1000	0.1
TH	Monoclonal/Mouse	N/A	EnCor	MCA-4H2	WB, ELISA, IHC	1:1000, 1:100	1
TH	Polyclonal/Rabbit	N/A	EnCor	RPCA-TH	WB, IHC	1:1000, 1:500	1
TH	Polyclonal/Rabbit	Biotin	EnCor	RPCA-TH	ELISA	1:6000	1.65
Chicken	Polyclonal/Rabbit	HRP	Sigma	A9046	WB	1:1000	1
Mouse	Polyclonal/Goat	IR-800	Licor	92632210	WB	1:15,000	0.0003
Rabbit	Polyclonal/Goat	IR-680	Licor	92568071	WB	1:15,000	0.0003
CD14	Nanobeads	Magnetic	Biolegend	480093	Magnetic Isolation	20 μL /20M cells	N/A
Biotin	N/A (Avidin)	HRP	Vector Labs	A2004	ELISA	1:2500	0.0004
Mouse	Polyclonal/Goat	HRP	Biolegend	405306	IHC	1:250	0.002
Isotype Ctl	IgG1,k/Mouse	N/A	Biolegend	401401	IHC, WB	1:250-1000	1
Isotype Ctl	Polyclonal/Rabbit	N/A	Biolegend	910801	IHC, WB	1:100-1000	1
Rabbit	Polyclonal/Donkey	HRP	Biolegend	406401	IHC	1:500-1000	0.002
CD14	Polyclonal	Magnetic	Biolegend	480048	ELISA, FC	Mfg Instr.	N/A
Ki67	Polyclonal/Chicken	N/A	Encor	CPCA-Ki67	FC	1:100	0.1
Chicken	Polyclonal/Goat	Alexa 488	LifeTech	A-11039	FC	1:100	0.2
CD14	IgG2b/Mouse	FITC	BD	M-Phi-09	FC	1:50	0.02

with vehicle, TPA (100 ng/mL, Biolegend, 755802)⁷, TNF α (17 ng/mL, Biolegend, 570102)⁶⁸, XPro1595 (50 ng/mL), or IL6 (17 ng/mL) in an ultra-low-adherence six-well plate (Corning, 3471) to prevent adherence. Suspended cells from each treatment group were aspirated and placed in a 15 mL conical tube, with any remaining adherent cells detached by incubation with 700 μL Accumax solution for 3 min (Innovative Cell Technologies, AM105) and added to suspended cells. After pelleting cells by centrifugation (3 min 100 \times g, room temperature), cells were assayed by either flow cytometry⁴⁷ or lysed for ELISA as stated above ("Preparation of cell lysates").

As previously published⁴⁷, cells for flow cytometry were fixed and permeabilized (eBioscience, 88-8824-00), and stained for intracellular marker TH (Millipore-Sigma, AB152, 1:100) followed by a species-specific secondary (anti-Rabbit BV421, BD, 565014). After resuspending the sample in a final volume of 250 μL PBS, 5 μL of Invitrogen CountBright Absolute Counting Beads (5000 beads/mL, Invitrogen, C36950) were added just prior to data acquisition (Sony Spectral Analyzer, SP6800). Monocytes were gated for single cells and positive TH expression (Fig. 5b), and normalized to counting beads in each sample to obtain an absolute count of TH⁺ monocytes per μL suspension.

Statistics

A two-tailed, unpaired *T* test was used to compare TH quantity in PD patients versus healthy control. In this experiment, $P < 0.05$ was considered statistically significant. One-way ANOVA with Tukey's correction for multiple comparisons was used to compare TH-expressing monocytes assayed by flow cytometry and ELISA following treatment with TPA, TNF α , XPro1595, IL6, or Vehicle. $P < 0.05$ was considered statistically significant.

Disclaimer

The content is solely the responsibility of the authors and does not necessarily represent the official views of the National Institutes of Health.

Reporting summary

Further information on research design is available in the Nature Research Reporting Summary linked to this article.

DATA AVAILABILITY

All data will be made available upon reasonable request.

Received: 16 March 2021; Accepted: 16 June 2021;
Published online: 20 July 2021

REFERENCES

- Molinoff, P. B. & Axelrod, J. Biochemistry of catecholamines. *Annu. Rev. Biochem.* **40**, 465–500 (1971).
- Nagatsu, T., Levitt, M., & Udenfriend, S. Tyrosine hydroxylase. The initial step in norepinephrine biosynthesis. *J. Biol. Chem.* **239**, 2910–2917 (1964).
- Berod, A., Biguet, N. F., Dumas, S., Bloch, B. & Mallet, J. Modulation of tyrosine hydroxylase gene expression in the central nervous system visualized by in situ hybridization. *Proc. Natl. Acad. Sci. USA* **84**, 1699–1703 (1987).
- Bertler, A. & Rosengren, E. Occurrence and distribution of catechol amines in brain. *Acta Physiol. Scand.* **47**, 350–361 (1959).
- Marino, F. et al. Endogenous catecholamine synthesis, metabolism storage, and uptake in human peripheral blood mononuclear cells. *Exp. Hematol.* **27**, 489–495 (1999).
- Cosentino, M. et al. Endogenous catecholamine synthesis, metabolism, storage and uptake in human neutrophils. *Life Sci.* **64**, 975–981 (1999).
- Cosentino, M. et al. Catecholamine production and tyrosine hydroxylase expression in peripheral blood mononuclear cells from multiple sclerosis patients: effect of cell stimulation and possible relevance for activation-induced apoptosis. *J. Neuroimmunol.* **133**, 233–240 (2002).
- Cosentino, M. et al. Interferon-gamma and interferon-beta affect endogenous catecholamines in human peripheral blood mononuclear cells: implications for multiple sclerosis. *J. Neuroimmunol.* **162**, 112–121 (2005).
- Matt, S. M. & Gaskill, P. J. Where is dopamine and how do immune cells see it?: dopamine-mediated immune cell function in health and disease. *J. Neuroimmune Pharmacol.* <https://doi.org/10.1007/s11481-019-09851-4> (2019).
- Weihe, E., Depboylu, C., Schütz, B., Schäfer, M. K. & Eiden, L. E. Three types of tyrosine hydroxylase-positive CNS neurons distinguished by dopa decarboxylase and VMAT2 co-expression. *Cell. Mol. Neurobiol.* **26**, 659–678 (2006).
- Harris, R. C. & Zhang, M. Z. Dopamine, the kidney, and hypertension. *Curr. Hypertens. Rep.* **14**, 138–143 (2012).

12. Wolfovitz, E. et al. Derivation of urinary dopamine from plasma dihydroxyphenylalanine in humans. *Clin. Sci.* **84**, 549–557 (1993).
13. Mohanty, P. K. et al. Myocardial norepinephrine, epinephrine and dopamine concentrations after cardiac autotransplantation in dogs. *J. Am. Coll. Cardiol.* **7**, 419–424 (1986).
14. Phaner, M. J., Galligan, J. J. & Swain, G. M. Increased catecholamine secretion from single adrenal chromaffin cells in DOCA-salt hypertension is associated with potassium channel dysfunction. *ACS Chem. Neurosci.* **4**, 1404–1413 (2013).
15. Leszczyszyn, D. J. et al. Secretion of catecholamines from individual adrenal medullary chromaffin cells. *J. Neurochem.* **56**, 1855–1863 (1991).
16. Wightman, R. M. et al. Temporally resolved catecholamine spikes correspond to single vesicle release from individual chromaffin cells. *Proc. Natl. Acad. Sci. USA* **88**, 10754–10758 (1991).
17. Gaskill, P. J., Carvallo, L., Eugenin, E. A. & Berman, J. W. Characterization and function of the human macrophage dopaminergic system: implications for CNS disease and drug abuse. *J. Neuroinflamm.* **9**, 203 (2012).
18. Cosentino, M. et al. Human CD4+CD25+ regulatory T cells selectively express tyrosine hydroxylase and contain endogenous catecholamines subserving an autocrine/paracrine inhibitory functional loop. *Blood* **109**, 632–642 (2007).
19. Lindgren, N. et al. Regulation of tyrosine hydroxylase activity and phosphorylation at Ser(19) and Ser(40) via activation of glutamate NMDA receptors in rat striatum. *J. Neurochem.* **74**, 2470–2477 (2000).
20. Kawahata, I. & Fukunaga, K. Degradation of tyrosine hydroxylase by the ubiquitin–proteasome system in the pathogenesis of Parkinson's disease and dopa-responsive dystonia. *Int. J. Mol. Sci.* **21**, <https://doi.org/10.3390/ijms21113779> (2020).
21. Congo Carbajosa, N. A. et al. Tyrosine hydroxylase is short-term regulated by the ubiquitin-proteasome system in PC12 cells and hypothalamic and brainstem neurons from spontaneously hypertensive rats: possible implications in hypertension. *PLoS ONE* **10**, e0116597 (2015).
22. Johnson, M. E., Salvatore, M. F., Maiolo, S. A. & Bobrovskaya, L. Tyrosine hydroxylase as a sentinel for central and peripheral tissue responses in Parkinson's progression: evidence from clinical studies and neurotoxin models. *Prog. Neurobiol.* **165–167**, 1–25 (2018).
23. Salvatore, M. F., Calipari, E. S. & Jones, S. R. Regulation of tyrosine hydroxylase expression and phosphorylation in dopamine transporter-deficient mice. *ACS Chem. Neurosci.* **7**, 941–951 (2016).
24. Wang, Y., Sung, C. C. & Chung, K. K. Novel enhancement mechanism of tyrosine hydroxylase enzymatic activity by nitric oxide through S-nitrosylation. *Sci. Rep.* **7**, 44154 (2017).
25. Daubner, S. C., Le, T. & Wang, S. Tyrosine hydroxylase and regulation of dopamine synthesis. *Arch. Biochem. Biophys.* **508**, 1–12 (2011).
26. Blanchard-Fillion, B. et al. Nitration and inactivation of tyrosine hydroxylase by peroxynitrite. *J. Biol. Chem.* **276**, 46017–46023 (2001).
27. Mogi, M. et al. Tumor necrosis factor- α (TNF- α) increases both in the brain and in the cerebrospinal fluid from Parkinsonian patients. *Neurosci. Lett.* **165**, 208–210 (1994).
28. Hirsch, E. C. et al. The role of glial reaction and inflammation in Parkinson's disease. *Ann. N. Y. Acad. Sci.* **991**, 214–228 (2003).
29. Harris, J. P. et al. Emerging regenerative medicine and tissue engineering strategies for Parkinson's disease. *NPJ Parkinsons Dis.* **6**, 4 (2020).
30. Foffani, G. & Obeso, J. A. A cortical pathogenic theory of Parkinson's disease. *Neuron* **99**, 1116–1128 (2018).
31. Ichinose, H. et al. Quantification of mRNA of tyrosine hydroxylase and aromatic L-amino acid decarboxylase in the substantia nigra in Parkinson's disease and schizophrenia. *J. Neural Transm. Parkinsons Dis. Dement. Sect.* **8**, 149–158 (1994).
32. Cosentino, M. et al. Stimulation with phytohaemagglutinin induces the synthesis of catecholamines in human peripheral blood mononuclear cells: role of protein kinase C and contribution of intracellular calcium. *J. Neuroimmunol.* **125**, 125–133 (2002).
33. Mogi, M. et al. Homospecific activity (activity per enzyme protein) of tyrosine hydroxylase increases in parkinsonian brain. *J. Neural Transm.* **72**, 77–82 (1988).
34. Kouchaki, E. et al. Increased serum levels of TNF- α and decreased serum levels of IL-27 in patients with Parkinson disease and their correlation with disease severity. *Clin. Neurol. Neurosurg.* **166**, 76–79 (2018).
35. Rathnayake, D., Chang, T. & Udagama, P. Selected serum cytokines and nitric oxide as potential multi-marker biosignature panels for Parkinson disease of varying durations: a case-control study. *BMC Neurol.* **19**, 56 (2019).
36. Qin, X. Y., Zhang, S. P., Cao, C., Loh, Y. P. & Cheng, Y. Aberrations in peripheral inflammatory cytokine levels in parkinson disease: a systematic review and meta-analysis. *JAMA Neurol.* **73**, 1316–1324 (2016).
37. McCoy, M. K. & Tansey, M. G. TNF signaling inhibition in the CNS: implications for normal brain function and neurodegenerative disease. *J. Neuroinflamm.* **5**, 45 (2008).
38. McCoy, M. K. et al. Blocking soluble tumor necrosis factor signaling with dominant-negative tumor necrosis factor inhibitor attenuates loss of dopaminergic neurons in models of Parkinson's disease. *J. Neurosci.* **26**, 9365–9375 (2006).
39. Lee, J. K., Tran, T. & Tansey, M. G. Neuroinflammation in Parkinson's disease. *J. Neuroimmune Pharm.* **4**, 419–429 (2009).
40. Su, X. et al. Synuclein activates microglia in a model of Parkinson's disease. *Neurobiol. Aging* **29**, 1690–1701 (2008).
41. Block, M. L. & Hong, J. S. Microglia and inflammation-mediated neurodegeneration: multiple triggers with a common mechanism. *Prog. Neurobiol.* **76**, 77–98 (2005).
42. Kim, Y. S. & Joh, T. H. Microglia, major player in the brain inflammation: their roles in the pathogenesis of Parkinson's disease. *Exp. Mol. Med.* **38**, 333–347 (2006).
43. Pickel, V. M., Joh, T. H., Field, P. M., Becker, C. G. & Reis, D. J. Cellular localization of tyrosine hydroxylase by immunohistochemistry. *J. Histochem. Cytochem.* **23**, 1–12 (1975).
44. Kastner, A., Hirsch, E. C., Herrero, M. T., Javoy-Agid, F. & Agid, Y. Immunocytochemical quantification of tyrosine hydroxylase at a cellular level in the mesencephalon of control subjects and patients with Parkinson's and Alzheimer's disease. *J. Neurochem.* **61**, 1024–1034 (1993).
45. Yan, H. Q. et al. Delayed increase of tyrosine hydroxylase expression in rat nigrostriatal system after traumatic brain injury. *Brain Res.* **1134**, 171–179 (2007).
46. Witkovsky, P., Gabriel, R. & Krizaj, D. Anatomical and neurochemical characterization of dopaminergic interplexiform processes in mouse and rat retinas. *J. Comp. Neurol.* **510**, 158–174 (2008).
47. Gopinath, A. et al. A novel approach to study markers of dopamine signaling in peripheral immune cells. *J. Immunol. Methods* **476**, 112686 (2020).
48. Giguere, N. et al. Increased vulnerability of nigral dopamine neurons after expansion of their axonal arborization size through D2 dopamine receptor conditional knockout. *PLoS Genet.* **15**, e1008352 (2019).
49. Colon-Perez, L. M. et al. Functional connectivity, behavioral and dopaminergic alterations 24 h following acute exposure to synthetic bath salt drug methylenedioxypyrovalerone. *Neuropharmacology* **137**, 178–193 (2018).
50. Contini, M. & Raviola, E. GABAergic synapses made by a retinal dopaminergic neuron. *Proc. Natl. Acad. Sci. USA* **100**, 1358–1363 (2003).
51. Feinstein, P., Bozza, T., Rodriguez, I., Vassalli, A. & Mombaerts, P. Axon guidance of mouse olfactory sensory neurons by odorant receptors and the beta2 adrenergic receptor. *Cell* **117**, 833–846 (2004).
52. Greene, L. A. & Tischler, A. S. Establishment of a noradrenergic clonal line of rat adrenal pheochromocytoma cells which respond to nerve growth factor. *Proc. Natl. Acad. Sci. USA* **73**, 2424–2428 (1976).
53. Graham, F. L., Smiley, J., Russell, W. C. & Nairn, R. Characteristics of a human cell line transformed by DNA from human adenovirus type 5. *J. Gen. Virol.* **36**, 59–74 (1977).
54. Shaw, G., Morse, S., Ararat, M. & Graham, F. L. Preferential transformation of human neuronal cells by human adenoviruses and the origin of HEK 293 cells. *FASEB J.* **16**, 869–871 (2002).
55. Saha, K. et al. Intracellular methamphetamine prevents the dopamine-induced enhancement of neuronal firing. *J. Biol. Chem.* **289**, 22246–22257 (2014).
56. Mackie, P. et al. The dopamine transporter: an unrecognized nexus for dysfunctional peripheral immunity and signaling in Parkinson's disease. *Brain Behav. Immun.* **70**, 21–35 (2018).
57. Miller, D. R. et al. Methamphetamine regulation of activity and topology of ventral midbrain networks. *PLoS ONE* **14**, e0222957 (2019).
58. Trudeau, L. E. et al. The multilingual nature of dopamine neurons. *Prog. Brain Res.* **211**, 141–164 (2014).
59. Morales, M. & Margolis, E. B. Ventral tegmental area: cellular heterogeneity, connectivity and behaviour. *Nat. Rev. Neurosci.* **18**, 73–85 (2017).
60. Caggiu, E. et al. Inflammation, infectious triggers, and Parkinson's disease. *Front. Neurol.* **10**, 122 (2019).
61. Kozina, E. et al. Mutant LRRK2 mediates peripheral and central immune responses leading to neurodegeneration in vivo. *Brain* **141**, 1753–1769 (2018).
62. Rentzos, M. et al. Circulating interleukin-15 and RANTES chemokine in Parkinson's disease. *Acta Neurol. Scand.* **116**, 374–379 (2007).
63. Brodacki, B. et al. Serum interleukin (IL-2, IL-10, IL-6, IL-4), TNF α , and INF γ concentrations are elevated in patients with atypical and idiopathic parkinsonism. *Neurosci. Lett.* **441**, 158–162 (2008).
64. Dufek, M. et al. Serum inflammatory biomarkers in Parkinson's disease. *Parkinsonism Relat. Disord.* **15**, 318–320 (2009).
65. Deleidi, M. & Gasser, T. The role of inflammation in sporadic and familial Parkinson's disease. *Cell Mol. Life Sci.* **70**, 4259–4273 (2013).
66. Jenei-Lanzl, Z. et al. Anti-inflammatory effects of cell-based therapy with tyrosine hydroxylase-positive catecholaminergic cells in experimental arthritis. *Ann. Rheum. Dis.* **74**, 444–451 (2015).

67. Miller, L. E., Grifka, J., Schölmerich, J. & Straub, R. H. Norepinephrine from synovial tyrosine hydroxylase positive cells is a strong indicator of synovial inflammation in rheumatoid arthritis. *J. Rheumatol.* **29**, 427–435 (2002).
68. Merry, K. & Gowen, M. The transcriptional control of TGF-beta in human osteoblast-like cells is distinct from that of IL-1 beta. *Cytokine* **4**, 171–179 (1992).
69. Doll, D. N., Rellick, S. L., Barr, T. L., Ren, X. & Simpkins, J. W. Rapid mitochondrial dysfunction mediates TNF-alpha-induced neurotoxicity. *J. Neurochem* **132**, 443–451 (2015).
70. Giustarini, G. et al. Tissue influx of neutrophils and monocytes is delayed during development of trovafloxacin-induced tumor necrosis factor-dependent liver injury in mice. *J. Appl. Toxicol.* **38**, 753–765 (2018).
71. Nakai, Y., Hamagaki, S., Takagi, R., Taniguchi, A. & Kurimoto, F. Plasma concentrations of tumor necrosis factor-alpha (TNF-alpha) and soluble TNF receptors in patients with anorexia nervosa. *J. Clin. Endocrinol. Metab.* **84**, 1226–1228 (1999).
72. Turner, D. A. et al. Physiological levels of TNFalpha stimulation induce stochastic dynamics of NF-kappaB responses in single living cells. *J. Cell Sci.* **123**, 2834–2843 (2010).
73. Damas, P. et al. Tumor necrosis factor and interleukin-1 serum levels during severe sepsis in humans. *Crit. Care Med.* **17**, 975–978 (1989).
74. Kim, K. H. & Sederstrom, J. M. Assaying cell cycle status using flow cytometry. *Curr. Protoc. Mol. Biol.* **111**, 28.26.21–28.26.11 (2015).
75. Pereira, J. R. et al. IL-6 serum levels are elevated in Parkinson's disease patients with fatigue compared to patients without fatigue. *J. Neurol. Sci.* **370**, 153–156 (2016).
76. Seppi, K. et al. Update on treatments for nonmotor symptoms of Parkinson's disease—an evidence-based medicine review. *Mov. Disord.* **34**, 180–198 (2019).
77. Lindqvist, D. et al. Non-motor symptoms in patients with Parkinson's disease—correlations with inflammatory cytokines in serum. *PLoS ONE* **7**, e47387 (2012).
78. Joers, V. et al. Microglia, inflammation and gut microbiota responses in a progressive monkey model of Parkinson's disease: a case series. *Neurobiol. Dis.* **144**, 105027 (2020).
79. O'Reilly, M. L. et al. Pharmacological inhibition of soluble tumor necrosis factor-alpha two weeks after high thoracic spinal cord injury does not affect sympathetic hyperreflexia. *J. Neurotrauma* <https://doi.org/10.1089/neu.2020.7504> (2021).
80. Braak, H. & Del Tredici, K. Invited Article: nervous system pathology in sporadic Parkinson disease. *Neurology* **70**, 1916–1925 (2008).
81. Goodwin, J. S. et al. Amphetamine and methamphetamine differentially affect dopamine transporters in vitro and in vivo. *J. Biol. Chem.* **284**, 2978–2989 (2009).
82. Swant, J. et al. alpha-Synuclein stimulates a dopamine transporter-dependent chloride current and modulates the activity of the transporter. *J. Biol. Chem.* **286**, 43933–43943 (2011).
83. Corkum, C. P. et al. Immune cell subsets and their gene expression profiles from human PBMC isolated by Vacutainer Cell Preparation Tube (CPT™) and standard density gradient. *BMC Immunol.* **16**, 48 (2015).
84. Flierl, M. A., Rittirsch, D., Huber-Lang, M., Sarma, J. V. & Ward, P. A. Catecholamines—crafty weapons in the inflammatory arsenal of immune/inflammatory cells or opening pandora's box? *Mol. Med.* **14**, 195–204 (2008).
85. Flierl, M. A. et al. Upregulation of phagocyte-derived catecholamines augments the acute inflammatory response. *PLoS ONE* **4**, e4414 (2009).
86. Torres, K. C. et al. Norepinephrine, dopamine and dexamethasone modulate discrete leukocyte subpopulations and cytokine profiles from human PBMC. *J. Neuroimmunol.* **166**, 144–157 (2005).
87. Kustrimovic, N. et al. Dopaminergic receptors on CD4+ T naive and memory lymphocytes correlate with motor impairment in patients with Parkinson's disease. *Sci. Rep.* **6**, 33738 (2016).
88. Bergquist, J., Tarkowski, A., Ekman, R. & Ewing, A. Discovery of endogenous catecholamines in lymphocytes and evidence for catecholamine regulation of lymphocyte function via an autocrine loop. *Proc. Natl. Acad. Sci. USA* **91**, 12912–12916 (1994).
89. Eugenin, E. A., Gaskill, P. J. & Berman, J. W. Tunneling nanotubes (TNT) are induced by HIV-infection of macrophages: a potential mechanism for intercellular HIV trafficking. *Cell. Immunol.* **254**, 142–148 (2009).
90. Nolan, R. & Gaskill, P. J. The role of catecholamines in HIV neuropathogenesis. *Brain Res.* **1702**, 54–73 (2019).

91. Nolan, R. A., Muir, R., Runner, K., Haddad, E. K. & Gaskill, P. J. Role of macrophage dopamine receptors in mediating cytokine production: implications for neuroinflammation in the context of HIV-associated neurocognitive disorders. *J. Neuroimmune Pharm.* **14**, 134–156 (2019).
92. Cartier, E. A. et al. A biochemical and functional protein complex involving dopamine synthesis and transport into synaptic vesicles. *J. Biol. Chem.* **285**, 1957–1966 (2010).

ACKNOWLEDGEMENTS

This work was funded by T32-NS082128 (to A.G.), National Center for Advancing Translational Sciences of the National Institutes of Health under University of Florida Clinical and Translational Science Awards TL1TR001428 and UL1TR001427 (to A.G.), R01NS071122-07A1 (to H.K.), NIDA Grant R01DA026947-10, National Institutes of Health Office of the Director Grant 15100D020026-01 (to H.K.), UF-Fixel Institute Developmental Fund, DA043895 (to H.K.), by the University of Florida McKnight Brain Institute (MBI) (to A.G.), by the Bryan Robinson Foundation (to A.G.) and by The Karen Toffler Charitable Trust (to A.G.). Illustrations made using Biorender© (Biorender.com).

AUTHOR CONTRIBUTIONS

M.F., M.B., G.S., A.C., D.R.M., C.A.H., A.D. and A.G., performed experiments, contributed written portions, figures and methods to this manuscript. P.M., M.G.T., I.M., A.R.-Z., M.S.O., W.J.S., H.K., and A.G., supervised, designed experiments in addition to direct contributions to the manuscript.

COMPETING INTERESTS

Malú Gámez Tansey is a co-inventor on the XPro1595 patent, and is a consultant to and has stock ownership in INmune Bio, which has licensed XPro1595 for neurological indications. The remaining authors declare no competing interests.

ADDITIONAL INFORMATION

Supplementary information The online version contains supplementary material available at <https://doi.org/10.1038/s41531-021-00201-x>.

Correspondence and requests for materials should be addressed to A.G.

Reprints and permission information is available at <http://www.nature.com/reprints>

Publisher's note Springer Nature remains neutral with regard to jurisdictional claims in published maps and institutional affiliations.



Open Access This article is licensed under a Creative Commons Attribution 4.0 International License, which permits use, sharing, adaptation, distribution and reproduction in any medium or format, as long as you give appropriate credit to the original author(s) and the source, provide a link to the Creative Commons license, and indicate if changes were made. The images or other third party material in this article are included in the article's Creative Commons license, unless indicated otherwise in a credit line to the material. If material is not included in the article's Creative Commons license and your intended use is not permitted by statutory regulation or exceeds the permitted use, you will need to obtain permission directly from the copyright holder. To view a copy of this license, visit <http://creativecommons.org/licenses/by/4.0/>.

© The Author(s) 2021, corrected publication 2021